ACS NANO

www.acsnano.org

ARTICLE

Can N95 Respirators Be Reused after Disinfection? How Many Times?

Lei Liao, Wang Xiao, Mervin Zhao, Xuanze Yu, Haotian Wang, Qiqi Wang, Steven Chu, and Yi Cui*

Cite This: https://dx.doi.org/10.1021/acsnano.0c03597

Read Online

ACCESS | Metrics & More | Article Recommendations | Supporting Information

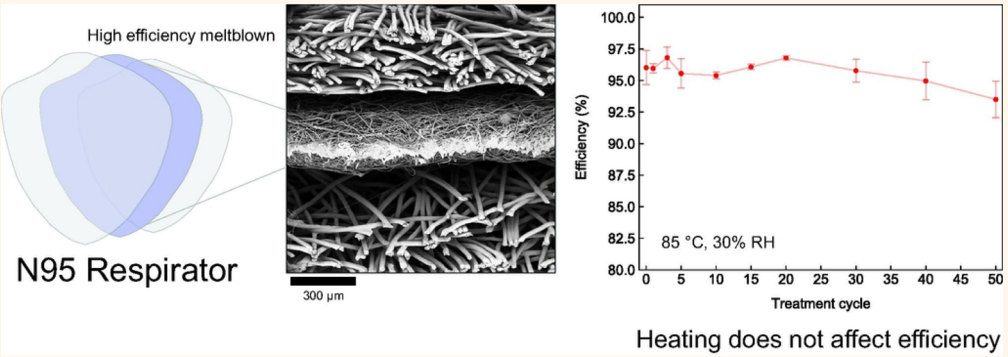

ABSTRACT: **The coronavirus disease 2019 (COVID-19) pandemic has led to a major shortage of N95 respirators, which are essential for protecting healthcare professionals and the general public who may come into contact with the virus. Thus, it is essential to determine how we can reuse respirators and other personal protective equipment in these urgent times. We investigated multiple commonly used disinfection schemes on media with particle filtration efficiency of 95%. Heating was recently found to inactivate the virus in solution within 5 min at 70 °C and is among the most scalable, user-friendly methods for viral disinfection. We found that heat (≤85 °C) under various humidities (≤100% relative humidity, RH) was the most promising, nondestructive method for the preservation of filtration properties in meltblown fabrics as well as N95-grade respirators. At 85 °C, 30% RH, we were able to perform 50 cycles of heat treatment without significant changes in the filtration efficiency. At low humidity or dry conditions, temperatures up to 100 °C were not found to alter the filtration efficiency significantly within 20 cycles of treatment. Ultraviolet (UV) irradiation was a secondary choice, which was able to withstand 10 cycles of treatment and showed small degradation by 20 cycles. However, UV can potentially impact the material strength and subsequent sealing of respirators. Finally, treatments involving liquids and vapors require caution, as steam, alcohol, and household bleach all may lead to degradation of the filtration efficiency, leaving the user vulnerable to the viral aerosols.**

KEYWORDS: *COVID-19, personal protective equipment, N95 reuse, disinfection, aerosol*

Coronavirus disease 2019 (COVID-19) is an ongoing pandemic with over three million confirmed cases and new cases increasing by ∼10% per day (at the time of writing)[1] that has caused major disruptions to nearly all facets of everyday life around the world. The disease is caused by the severe acute respiratory syndrome coronavirus 2 (SARS-CoV-2), which was first detected in Wuhan, China.[2,3] The virus is likely of zoonotic origin and, like the SARS-CoV, enters human cells *via* the angiotensin-converting enzyme 2 (ACE2). ACE2 is a membrane protein that is responsible for regulating vasoconstriction and blood pressure and serves as an entry point for coronaviruses found in the lungs, heart, kidneys, and intestines. SARS-CoV-2 utilizes ACE2 more efficiently than does SARS-CoV, which may explain why the human-to-human transmissibility of COVID-19 is so high.[4]

Once infected, the patient exhibits flu-like symptoms such as fever, chest tightness, dry cough, and, in some cases, severe pneumonia and acute respiratory distress syndrome (ARDS) develops.[5−8] Because the incubation period is *ca.* 3−4 days but

Received: April 29, 2020
Accepted: May 1, 2020

https://dx.doi.org/10.1021/acsnano.0c03597
ACS Nano XXXX, XXX, XXX−XXX

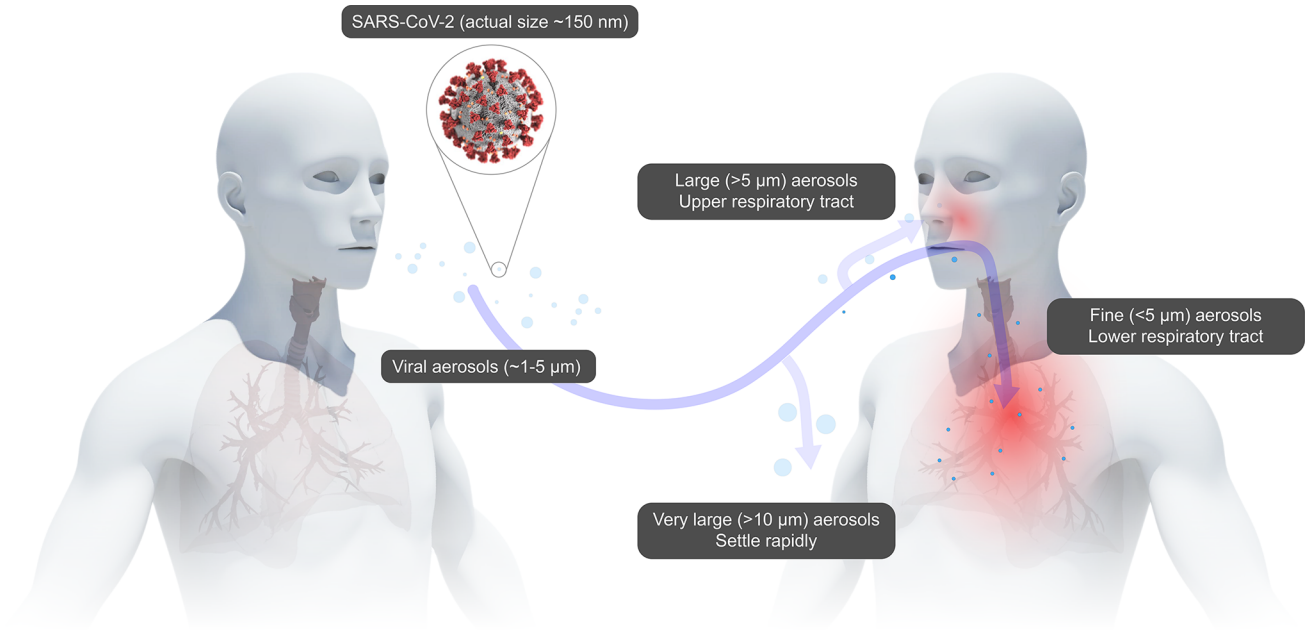

Figure 1. Transmission of SARS-CoV-2 through viral aerosols. Image of SARS-CoV-2 courtesy of the CDC.

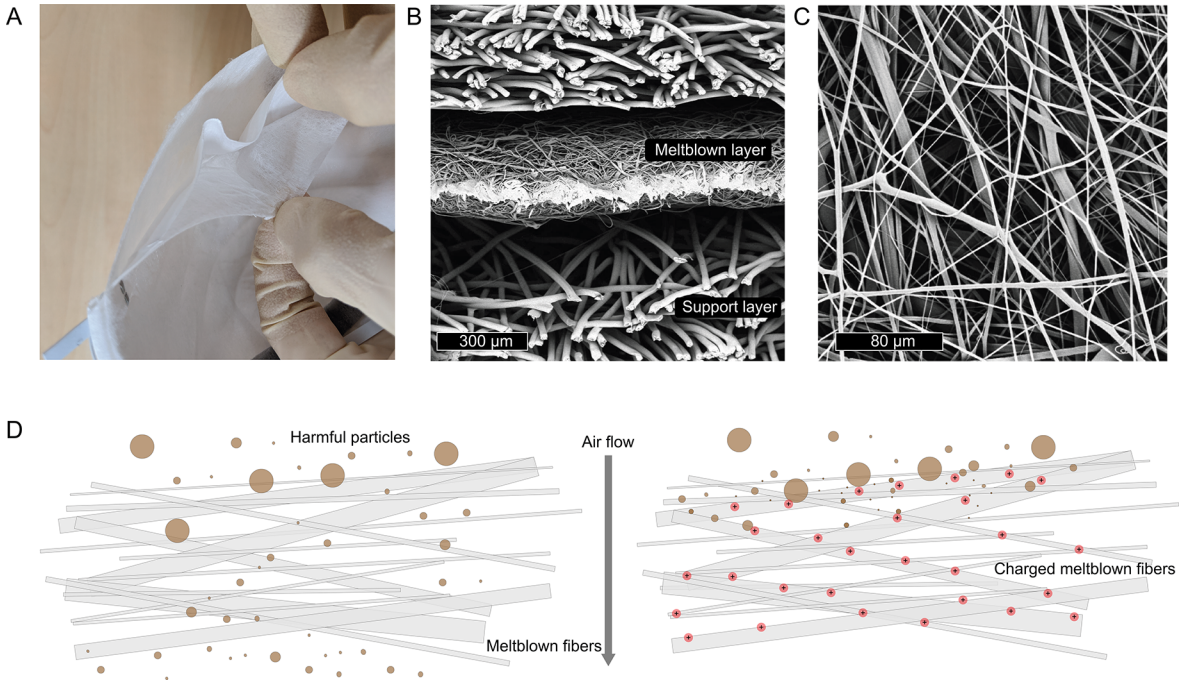

Figure 2. Meltblown fabrics in N95 FFRs. (A) Peeling apart a representative N95 FFR reveals multiple layers of nonwoven materials. (B) Scanning electron microscope (SEM) cross-section image reveals the middle meltblown layer has thinner fibers with thickness around 300 μm. (C) SEM image of meltblown fibers reveals a complicated randomly oriented network of fibers, with diameters in the range of ~1−10 μm. (D) Schematic illustration of meltblown fibers (left) without and (right) with electret charging. In the left figure, smaller particles are able to pass through to the user, but particles are electrostatically captured in the case of an electret (right).

can be as long as 20 days, along with the presence of asymptomatic carriers, the virus has been extremely difficult to contain.[9] Although the initial mortality rate was estimated to be *ca.* 3.5% in China, compounding the longer incubation period and testing delays has led to new global estimates of *ca.* 5.7%.[10]

Although the precise mode SARS-CoV-2's viral transmission is not known, a primary transmission mode in viruses such as SARS and influenza is through short-range aerosols and droplets.[11] When a person infected with a virus breathes, speaks, sings, coughs, or sneezes, micron-sized aerosols containing the virus are released into the air. Data gathered from influenza patients suggest that these aerosols are typically fine (<5 μm) or coarse (>5 μm).[11−13] Coarse particles can settle due to gravity within 1 h. Fine particles, however, especially those smaller than 1 μm, can essentially stay in the air nearly indefinitely. Droplets, or particles >10 μm, settle rapidly and are not typically deposited in the respiratory tract

https://dx.doi.org/10.1021/acsnano.0c03597
ACS Nano XXXX, XXX, XXX−XXX

through means of aerosol inhalation. Particles larger than 5 μm typically only reach the upper respiratory tract, whereas fine particles <5 μm are critically able to reach the lower respiratory tract, similar to harmful particulate matter pollution (Figure 1). Although coughing and sneezing provide many aerosols, the size distribution and number of particles emitted during normal speech serve as a significant viral transmitter.[12] Singing has been found to be comparable to continuous coughing in the transmission of airborne pathogens,[14] which was demonstrated during a choir practice on March 10, 2020 in Washington state. Although the choir members did not touch each other or share music during the rehearsal, 45 out of the 60 members of the Skagit Valley Choir were diagnosed with the virus 3 weeks later, and two had died.

For dangerous airborne particulates, including viral aerosols during the current COVID-19 pandemic, the United States Centers for Disease Control and Prevention (CDC) recommends the usage of N95 filtering facepiece respirators (FFR) as personal protective equipment for healthcare professionals.[15−17] The N95 grade is determined by the CDC's National Institute of Occupational Safety and Health (NIOSH) (document 42 CFR Part 84), which designates a minimum filtration efficiency of 95% for 0.3 μm (aerodynamic mass mean diameter) of sodium chloride aerosols. In addition to N95, there are N99 and N100 standards, which correspond to filtration efficiencies of 99% and 99.97%, respectively. For oil-based aerosols (DOP), NIOSH also has created grades R and P (with filtration efficiencies 95−99.97%). Elsewhere around the globe, the equivalent filtration grades to N95 are FFP2 (European Union), KN95 (China), DS/DL2 (Japan), and KF94 (South Korea). Although the actual SARS-CoV-2 virus is *ca.* 150 nm,[18] commonly found N95 respirators can offer protection against particles as small as 80 nm with 95% filtration efficiency (initial testing, not loaded).[19] With the actual viral aerosols in the ∼1 μm range, the N95 FFRs' filtration efficiency should be sufficient for personal protection.

The N95 FFR is composed of multiple layers of, typically, polypropylene nonwoven fabrics (Figure 2A).[20] Among these layers, the most critical is that which is produced by the meltblown process. In typical FFRs, the meltblown layer is 100−1000 μm in thickness and composed of polypropylene microfibers with diameters in the range of ∼1−10 μm, as seen in the scanning electron microscope (SEM) images in Figure 2B,C. Due to the production method, meltblown fibers produce a lofty nonwoven material where the fibers can stack and create a three-dimensional network that has a porosity of 90%,[21] leading to high air permeability.

However, given that the fiber diameters are relatively small and the filters' void space is large, the filtration efficiencies of meltblown fabrics by themselves should not be adequate for fine particle filtration (Figure 2D). To improve the filtration efficiency while keeping the same high air permeability, these fibers are charged through corona discharge and/or triboelectric means into quasi-permanent dipoles called electrets.[22,23] Once they are charged, the filter can significantly increase its filtration efficiency without adding any mass or density to the structure. In addition, whereas other filter media may decrease in efficiency when loading the filter with more aerosol (NaCl, DOP), the meltblown electrets are able to keep a relatively consistent efficiency throughout the test.[24]

The COVID-19 pandemic has led to a significant shortage of N95 FFRs,[25] especially among healthcare providers. Although the virus will eventually become inactive on the mask surface and it is unlikely to penetrate fully to the user's intake side, a recent study shows that 72 h were required for the concentration of SARS-CoV-1 and SARS-CoV-2 viruses on plastic surfaces (40% RH and 21−23 °C) to be reduced by 3 orders of magnitude (from $10^{3.7}$ to $10^{0.6}$ $TCID_{50}$ per mL of medium).[26] Assuming a similar longevity on FFR surfaces, it is important to develop procedures for the safe and frequent reuse of FFRs without reducing the filtration efficiency. The CDC has recommended many disinfection or sterilization methods, typically involving chemical, radiative, or temperature treatments.[27] In brief, the mechanisms of disinfection or sterilization of bacteria and viruses include protein denaturation (alcohols, heat), DNA/RNA disruption (UV, peroxides, oxidizers), and cellular disruption (phenolics, chlorides, aldehydes). Although none of these methods have been extensively evaluated for SARS-CoV-2 inactivation specifically, we tested methods that can be easily deployed within a hospital setting, and possibly accessible for the general population, with relatively high throughput for FFR reuse.

RESULTS

Among the CDC forms of disinfection, we chose five commonly used and potentially scalable, user-friendly methods: (1) heat under various humidities (heat denaturation inactivates SARS-CoV with temperatures >65 °C in solution, and possibly SARS-CoV-2 with temperatures >70 °C for 5 min);[28−30] (2) steam (100 °C heat-based denature); (3) 75% alcohol (denaturing of the virus, based on the CDC); (4) household diluted chlorine-based solution (oxidative or chemical damage, based on the CDC); and (5) ultraviolet germicidal irradiation (UVGI was able to inactivate the SARS-CoV in solution with UV−C light at a fluence of ∼3.6 J/cm^2).[28] An oven, a UV−C sterilizer cabinet (found in barbershops or salons), steam, or liquid sprays can all realistically be deployed in the modern hospital setting and potentially in homes if needed. We did not consider some other common but more inaccessible techniques (equipment such as electron beam irradiation or plasma generators can be expensive or dangerous) or techniques known to cause damage to the FFR.[31]

Due to the shortage of FFRs, data collected were tested on a meltblown fabric (20 g/m^2) with initial efficiency ≥95% (full details are listed in the Methods), unless otherwise specified. These samples are representative of how the filtration efficiency in a N95 FFR may change given exposure to these treatments in the worst-case scenario (*i.e.*, no protective layer of the FFR). All meltblown samples were characterized using an industry standard Automated Filter Tester 8130A (TSI, Inc.) with a flow rate of 32 L/min and NaCl aerosol (0.26 μm mass median diameter). We subjected the meltblown samples to the aforementioned five disinfection methods and summarized the data in Table 1.

From the first disinfection, we can clearly note that the solution-based methods (ethanol and chlorine-based solution) drastically degraded the filtration efficiency to unacceptable levels, while the pressure drop remained comparable. As the pressure drop remained constant, this indicated that the loftiness and structure of the meltblown were unchanged, and the resultant efficiency degradation is the result of less apparent static charge on the electret (Figure S1). It is hypothesized in the literature that small molecules such as solvents can adsorb onto the fabrics' fibers and either screen or possibly lift the frozen charges of the electret,[32] which would

https://dx.doi.org/10.1021/acsnano.0c03597
ACS Nano XXXX, XXX, XXX−XXX

Table 1. One-Time Disinfection Treatment on a Meltblown Fabric[a]

treatment	mode of application	treatment time (min)	filtration efficiency (%)	pressure drop (Pa)
initial samples			96.52 ± 1.37	8.7 ± 1.0
dry heat (75 °C)	static-air oven	30	96.67 ± 0.65	6.0 ± 1.0
steam	beaker of boiling water	10	95.16 ± 0.73	9.0 ± 1.0
ethanol (75%)	immersion and air dry	until dry	56.33 ± 3.03	7.7 ± 0.6
chlorine-based (2%)	light spray and air dry	5	73.11 ± 7.32	9.0 ± 1.0
UVGI (254 nm, 8 W)	sterilization cabinet	30	95.50 ± 1.59	7.0 ± 0.0

[a]The data from the initial samples displayed here are used throughout the remainder of the text and represent the mean and standard deviation from 30 samples. For all other data here, three samples were used for each initial treatment.

decrease the filtration efficiency. In the case of disinfection with ethanol-based solutions, recent preliminary work also shows that vacuum drying may be able to restore the efficiency of FFRs.[33] It is also possible that the chlorine-based solution may degrade the efficiency less than the alcohol-based solution due to the higher water content. As polypropylene is hydrophobic, the chlorine-based solution may have a more difficult time penetrating the fabric and the static charge of fibers deeper within the meltblown may be less affected.

These initial results are mostly in agreement with a NIOSH-published report regarding the decontamination of whole FFRs,[34] though it placed more focus on gas-based methods, which could be suitable to well-controlled industrial-scale disinfection. However, this may not be practical for on-site disinfection within the current hospital and clinic infrastructure. The report found that bleach (immersion in a diluted solution) resulted in less of a drop in efficiency than our results indicated, but the authors noted that there were strong odors from off-gassing, which is another reason to exclude this as a method to consider for the end-user.

We chose to focus on the three remaining treatment methods to perform multiple treatment cycles. The meltblown fabrics after 10 cycles of each treatment are summarized in Figure 3 (data provided in Table S1). After three treatments of these three methods, the meltblown fabric still has characteristics similar to the initial sample. However, after five steam treatments, the efficiency has a sharp drop which continues at cycle 10 (Table S2). Similar to the alcohol- and chlorine-solution treatments, the pressure drop can be maintained at ∼8−9 Pa, but the efficiency degrades to around ∼80%, which would be concerning in an environment with high viral aerosol concentrations. As with the solution treatments, the pressure drops remained similar, which suggests it is also due to the decay of static charge. The dwelling time and frequency may be critical for how well the static charge can be preserved. If steam treatments saturate the fibers many times and condense water droplets on the fibers, it is possible that the static charge decays after multiple treatments. Because this decay is due to the direct water molecule contact with the fibers, it may be possible to alleviate the static decay if the fibers do not come into contact with the vapor directly (sealed container, apparatus, bag, *etc.*) and steam only serves as the heating element.

Given that steam also resulted in eventual efficiency degradation, we further determined the limits of temperature and humidity. We performed multiple humidity experiments (30%, 70%, and 100% RH) at 85 °C (20 min/cycle) and observed no appreciable degradation of efficiency at any humidity level (Figure 4A,B). At 85 °C, 30% RH, we observed no efficiency degradation over 50 cycles on a meltblown fabric (Figure 4C,D). Using less harsh conditions (75 °C, dry heat), the results are expectedly in agreement (Figure S2). These results are further confirmed when testing multiple N95-level FFRs from various countries (listed in Methods) at 85 °C, 30% and 100% RH for 20 cycles (Figure 4E,F). Testing conditions for the FFRs were under a flow rate of 85 L/min. From all the FFRs, we observed little change in the filtration properties, as all FFRs with filtration efficiency >95% were able to retain filtration efficiencies >95% after 20 cycles of heat treatment, even in a humid environment.

To determine the upper limit of applicable temperature, we tested low humidity conditions (≤30% RH) up to 125 °C (10 min/cycle), plotted in Figure 4G,H (data provided in Table S3), as higher temperatures should lead to a shorter minimum treatment time and an increase in the method turnover speed. There is little to no change in the filtration efficiency and pressure drop up to 100 °C in low-moisture conditions. However, at 125 °C, there is a sharp drop in the filtration efficiency while maintaining a constant pressure drop at around

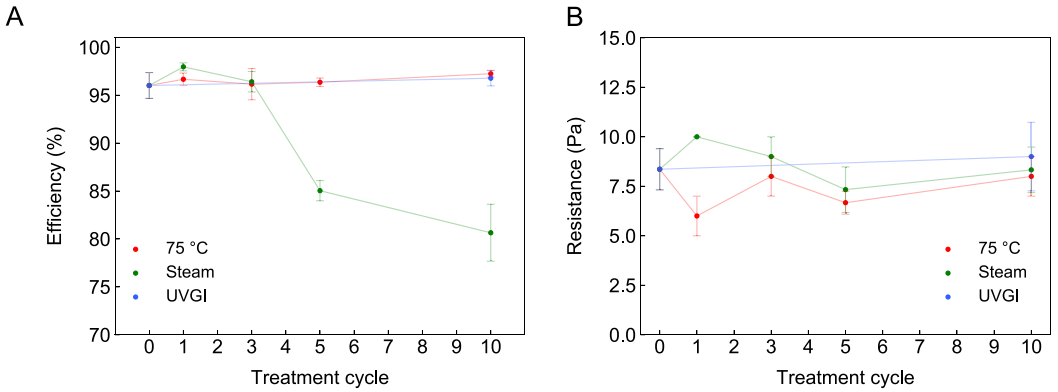

Figure 3. The 10 treatment cycle evolution of filtration characteristics. (A) Efficiency evolution where it is clear that steam treatment results in a degradation of efficiency. (B) Pressure drop evolution where it is not apparent that any structure or morphology change has occurred in the meltblown fabrics.

https://dx.doi.org/10.1021/acsnano.0c03597
ACS Nano XXXX, XXX, XXX−XXX

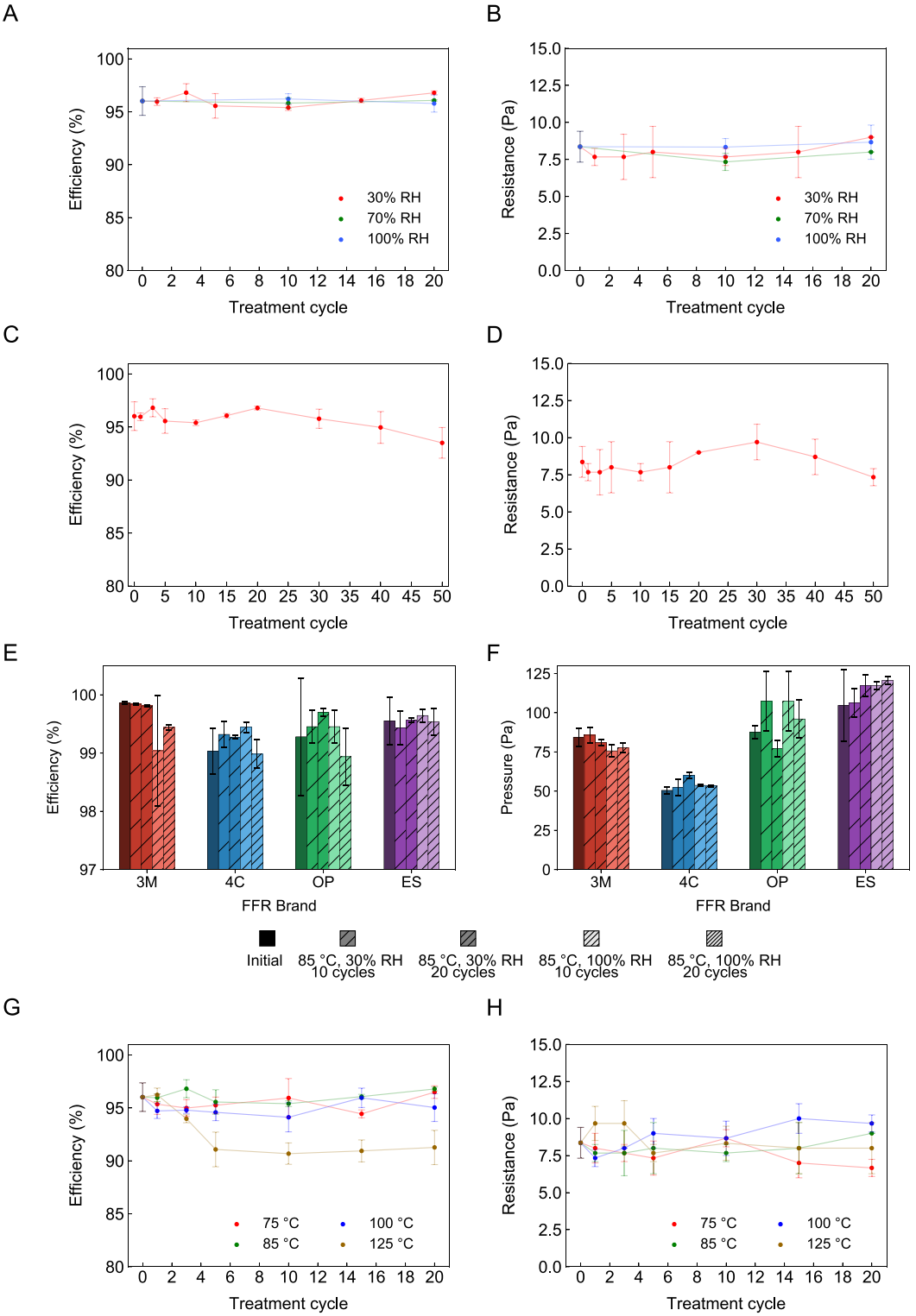

Figure 4. Temperature and humidity evolution of meltblown and FFR filtration characteristics. (A, B) Evolution of meltblown fabrics' filtration characteristics at 85 °C under different humidities, efficiency (A) and pressure drop (B). (C, D) Evolution of filtration characteristics on a meltblown fabric under 85 °C, 30% RH, efficiency (C) and pressure drop (D). (E, F) Evolution of the filtration characteristics on an N95-level FFRs with 85 °C, under 30% and 100% RH (measured at a flow rate of 85 L/min), efficiency (E) and pressure drop (F). The left-to-right of all FFR brands is as follows: (1) initial (leftmost, solid pattern, tested in ambient conditions), (2) 85 °C, 30% RH 10 cycles, (3) 85 °C, 30% RH 20 cycles, (4) 85 °C, 100% RH 10 cycles, and (5) 85 °C, 100% RH 20 cycles. (G, H) Temperature dependence of meltblown fabrics' filtration characteristics over 20 cycles with RH < 30%, efficiency (G) and pressure drop (H).

cycle 5. Similarly, the lack of pressure drop change indicates that the degradation is also due to the static decay. Considering the higher temperature, polypropylene's melting point (130−170 °C), as well as the thin and fibrous nature of the media, it is possible that the higher temperature is enough to relax the microscopic charge state within the polymer,

https://dx.doi.org/10.1021/acsnano.0c03597
ACS Nano XXXX, XXX, XXX−XXX

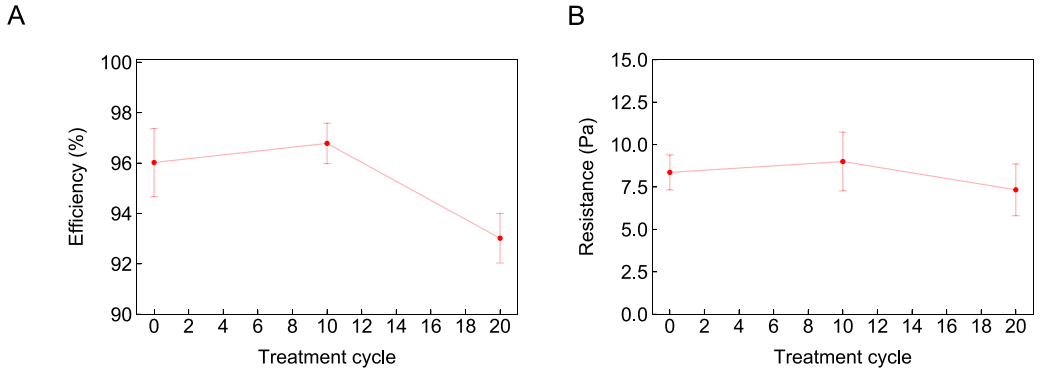

Figure 5. Effect of UVGI on meltblown filtration characteristics. (A) Efficiency of meltblown fabric that slightly changes after 10 cycles of UVGI. (B) Pressure drop after UVGI treatments remains similar. The larger error bar in the initial data is due to the meltblown fabric originating from various locations on the roll, whereas the meltblown fabrics used in the treatment originated from a similar location on the roll.

resulting in some of the quasi-stable polarization to become depolarized to their neutral state. From SEM images, we did not identify any morphological changes and did not observe any apparent physical deformations (Figure S3), which may support this conclusion. This effect is not as strong as direct solvent contact, which reduced the filtration efficiency to <80%, whereas 125 °C reduced the efficiency to ∼90%. The mechanism of efficiency degradation may differ, as the solvent may form molecular adsorption layers or possibly liberate charge traps, but higher temperatures provide energy to return some of the fibers' polarized state to a relaxed state.

Heat was a promising scalable method that may be suitable for FFR reuse. We can conclude that the highest subjectable temperature to the FFR for repeated use with ≥95% efficiency is <100 °C. At temperatures of ≤85 °C, humidity does not seem to play a crucial role in the filtration properties, as FFRs tested at a near 100% RH at 85 °C were unaffected. However, as steam results in a decrease in efficiency, the humidity should be kept low if approaching 100 °C. The temperature range here may pose some limitations in the available equipment, but we believe the current hospital infrastructure, and possibly the general population, should be able to perform these treatments. This includes using dryers, ovens, circulators, or even hot air guns, all of which are relatively scalable and user-friendly. Although the most common method to inactivate SARS-CoV-2 in solution is 56 °C for 30 min in a laboratory setting,[35] repeated treatments at temperatures below 65 °C (30 min) is not advised, as it was the reported temperature required to inactivate SARS-CoV in solution and limit it to undetectable traces.[29] Because these prior inactivation tests occurred in solution, further study on the heat inactivation of aerosolized viruses is required.

It is important to note that the real-world use of FFRs may lead to contamination of the nonwoven layers with sweat and/or oral droplets (dirt, salts, or other chemicals/particles), which may negatively impact the efficiency (adsorption, charge degradation, or even physical damage after prolonged periods). If these contaminants impact the electrostatic ability of the respirator, the heat treatment would not be able to restore this charge and would, at best, keep the efficiency as is. Further work may be needed to test the degradation of efficiency after use and if such heating procedures on used FFRs are changed by the introduction of these usage-incurred contaminants.

Finally, we tested the effect of UVGI on meltblown samples up to 20 cycles (Figure 5). The UVGI sterilization cabinet here provides UV−C light centered at a wavelength of 254 nm with an intensity of 8 W. The UV−C light areal intensity distribution is not uniform inside the cabinet, and its exact value needs to be measured in the future for dose determination, as the necessary radiation to inactivate SARS-CoV was previously found to be above ∼3.6 J/cm^2.[28] At 10 cycles, the data are in agreement with the NIOSH report,[34] but efficiency eventually decays to 93% at 20 cycles, making it unsuitable for N95-grade FFRs by itself.

Although UV radiation may possess enough energy to break the chemical bonds and degrade polypropylene, the dosage of the sterilization chamber is relatively low, and the material degrades slowly. This finding is supported by previous experiments that showed UV−C doses up to 950 J/cm^2 did not appreciably change the filtration efficiency.[36] A possible concern regarding UVGI disinfection for FFRs relates to the UV penetration depth. Because UV−C has a wavelength around 250 nm and polypropylene is a UV absorber, it is difficult to conclude if smaller viral particles deep within the filter can be deactivated through UVGI. If the particles are of a larger size and remain localized on the surface, UVGI may be a candidate for FFR reuse. Furthermore, this means that UVGI requires FFRs not to be stacked, as the incident radiation will only be absorbed by the topmost surface. Another disadvantage is that UVGI was reported to significantly impact the mechanical strength of some FFRs with doses of around 1000 J/cm^2.[36]

Therefore, UVGI may be a useful disinfection technique, but the exact exposure or intensity of the UV−C light fluence on the mask surface would need to be verified. The variation in UVGI intensity has been the cause of discrepancies in the literature, as 3M's own internal reports recently showed that their UVGI treatments damaged particular FFRs,[37] whereas other reports show that UVGI cycling on multiple N95 FFRs had minimal or no impact.[31]

Most of our tests were performed on meltblown fabrics with an initial efficiency of >95% due to the current shortage of FFRs, leaving concern over whether other FFR components (straps, valves, nosepiece, foam, *etc.*) can change in these treatment environments. These components can impact the fit and sealing of the FFR, which is equally important as the FFR efficiency itself. From our experiments, we also used typical N95-grade FFRs to test the strap elasticity and structural integrity after heat treatments. We noted no apparent or qualitative change in the strap elasticity or fit compared with

https://dx.doi.org/10.1021/acsnano.0c03597
ACS Nano XXXX, XXX, XXX−XXX

the untreated model for the heat treatments, and quantitative studies confirmed this finding.[38] Although no qualitative damage was observed on the UV-treated FFRs, quantitative tests revealed that UVGI treatments at this dosage can lead to improper fitting.[38]

Because actually donning and using the respirator impacts the structural stability of such components, particular care needs to be taken in the interpretation of these results. Previous reports indicated that FFRs can safely be worn up to five times, but beyond five times may result in a less-than-adequate fit.[39] During this crisis, users have to make sure that the fit of the FFRs after treatment is adequate and that they are not left vulnerable due to leakage. Mask producers or users may need to consider straps that are more robust for reuse or that can withstand treatment conditions.

CONCLUSIONS

In conclusion, COVID-19 is an extremely contagious disease that requires healthcare professionals to take caution with necessary protective equipment. The current shortage of N95 FFRs during this time of rapidly spreading infection may be mitigated by methods that will enable their safe reuse. We tested methods that may be suitable for the reuse of particulate respirators and hope our results will be useful in helping hospitals, health care facilities, and the public in formulating safe standard operating procedures so that virus inactivation is assured while not compromising mask protection. We reiterate that although these methods were not tested on FFRs that have been exposed to SARS-CoV-2, these methods use disinfection precedents set by either SARS-CoV or recent data based on inactivation of SARS-CoV-2 in solution. We found that of commonly deployable methods, heating (dry or in the presence humidity) <100 °C can preserve the filtration characteristics of a pristine N95 respirator. The UVGI (254 nm, 8 W) sterilizer cabinet used in these tests does not have enough dose to impact the filtration properties within a reasonable number of treatment cycles and may be considered for disinfection, however the exact dose output of the cabinet would need to be determined such that it is suitable for inactivation of SARS-CoV-2 with minimal FFR damage. Using steam to disinfect requires caution, as the treatments may seem to be suitable, but prolonged treatment may leave the user with unsuitable protection. Finally, we advise against liquid contact, such as alcohol solutions, chlorine-based solutions, or soaps to clean the respirator, as this will lead to a degradation in the static charge that is necessary for the FFR to meet the N95 standard.

METHODS

Sample Preparation. Meltblown fabric was procured from Guangdong Meltblown Technology Co., Ltd. under the sample name TM95 with a 20 g/m^2 basis weight and initial filtration efficiency of ≥95%. All of the meltblown samples used were from this source. Each sample was cut to approximately 15 cm × 15 cm. All sample testing was performed on an Automated Filter Tester 8130A (TSI, Inc.) using a flow rate of 32 L/min and NaCl as the aerosol (0.26 μm mass median diameter). Each average measurement contains at least three individual sample measurements.

We chose disposable N95-grade FFRs for testing: 3M 8210 (NIOSH N95), 4C Air, Inc. (GB2626 KN95), ESound (GB2626 KN95), and Onnuriplan (KFDA KF94). These FFRs are referred to as "3M", "4C", "ES", and "OP", respectively, in figures. Full FFR testing used a flow rate of 85 L/min.

Scanning electron microscope images were recorded using a Phenom Pro SEM, at 10 kV.

Heat Treatment. Samples were loaded into a preheated five-sided heating chamber (Across International, LLC or SH-642, ESPEC) at the temperatures and times given in the main text. Dry heat was applied using the Across International vacuum heating oven under ambient conditions. In the case of the SH-642, the humidity was set to the lowest value (30% RH up to 85 °C; above 85 °C, the humidity is <30% but cannot be controlled). High humidity (100% RH) was simulated *via* sealing meltblown fabrics, or FFRs, inside a polyethylene bag with 0.3 mL of water and placing them inside the SH-642 chamber. The resting time between cycles was 10 min for the 75 and 85 °C treatments and 5 min for the 100 and 125 °C treatments. After resting, the samples were returned to the chamber to begin the next cycle. We initially chose 75 °C due to the presence of blanket warming ovens in hospital environments that can reach ∼80 °C. Further experiments used 85 °C, in the event that 75 °C is insufficient to inactivate SARS-CoV-2. Microwaving was not considered as many FFRs contain metals which may spark and melt the fabric.

Steam Treatment. Three samples were stacked on top of a beaker with boiling water inside (at around 15 cm above the water). The samples were left on top of the beaker and steamed for 10 min, and afterward they were left to air-dry completely (to touch). Samples were either tested or placed back on top of the beaker to continue the next treatment cycle.

Alcohol Treatment. Samples were immersed into a solution of 75% ethanol and left to air-dry (hanging) and subsequently tested.

Chlorine Solution Treatment. Samples were sprayed with approximately 0.3−0.5 mL of household chlorine-based disinfectant (∼2% NaClO). Samples were left to air-dry and off-gas completely,-while hanging. Samples were tested.

UVGI. Samples were placed into a UV sterilizer cabinet (CHS-208A), with a 254 nm, 8 W lamp, and 475 cm^2 internal area. Samples were irradiated for 30 min and left to stand under ambient conditions for 10 min per cycle. Samples were either returned to the chamber for the next cycle or tested.

ASSOCIATED CONTENT

Supporting Information

The Supporting Information is available free of charge at https://pubs.acs.org/doi/10.1021/acsnano.0c03597.

Additional SEM images, plots, and tables with compiled data (PDF)

AUTHOR INFORMATION

Corresponding Author

Yi Cui − *Department of Materials Science and Engineering, Stanford University, Stanford, California 94305, United States; Stanford Institute for Materials and Energy Sciences, SLAC National Accelerator Laboratory, Menlo Park, California 94025, United States;* orcid.org/0000-0002-6103-6352; Email: yicui@stanford.edu

Authors

Lei Liao − *4C Air, Inc., Sunnyvale, California 94089, United States*

Wang Xiao − *4C Air, Inc., Sunnyvale, California 94089, United States*

Mervin Zhao − *4C Air, Inc., Sunnyvale, California 94089, United States;* orcid.org/0000-0002-7313-7150

Xuanze Yu − *4C Air, Inc., Sunnyvale, California 94089, United States*

Haotian Wang − *4C Air, Inc., Sunnyvale, California 94089, United States*

Qiqi Wang − *4C Air, Inc., Sunnyvale, California 94089, United States*

https://dx.doi.org/10.1021/acsnano.0c03597
ACS Nano XXXX, XXX, XXX−XXX

Steven Chu − *Department of Physics and Department of Molecular and Cellular Physiology, Stanford University, Stanford, California 94305, United States*

Complete contact information is available at: https://pubs.acs.org/10.1021/acsnano.0c03597

Author Contributions

L.L. and Y.C. designed the experiments. L.L., W.X., M.Z., X.Y., and H.W. collected the data. L.L., M.Z., Q.W., and Y.C. analyzed the data and interpreted results. M.Z., L.L., Q.W., Y.C., and S.C. wrote the manuscript.

Notes

The authors declare the following competing financial interest(s): Professors Steven Chu and Yi Cui are founders and shareholders of the company 4C Air, Inc. They are inventors on patent PCT /US2015/065608. All other authors are employees of 4C Air, Inc.

ACKNOWLEDGMENTS

We would like to thank L. Chu and A. Price at Stanford Medicine for the helpful discussion.

REFERENCES

(1) Dong, E.; Du, H.; Gardner, L. An Interactive Web-Based Dashboard to Track COVID-19 in Real Time. *Lancet Infect. Dis.* **2020**, *20*, 533−534.

(2) Zhou, P.; Yang, X.-L.; Wang, X.-G.; Hu, B.; Zhang, L.; Zhang, W.; Si, H.-R.; Zhu, Y.; Li, B.; Huang, C.-L.; Chen, H.-D.; Chen, J.; Luo, Y.; Guo, H.; Jiang, R.-D.; Liu, M.-Q.; Chen, Y.; Shen, X.-R.; Wang, X.; Zheng, X.-S.; et al. A Pneumonia Outbreak Associated with a New Coronavirus of Probable Bat Origin. *Nature* **2020**, *579*, 270−273.

(3) Wu, F.; Zhao, S.; Yu, B.; Chen, Y.-M.; Wang, W.; Song, Z.-G.; Hu, Y.; Tao, Z.-W.; Tian, J.-H.; Pei, Y.-Y.; Yuan, M.-L.; Zhang, Y.-L.; Dai, F.-H.; Liu, Y.; Wang, Q.-M.; Zheng, J.-J.; Xu, L.; Holmes, E. C.; Zhang, Y.-Z. A New Coronavirus Associated with Human Respiratory Disease in China. *Nature* **2020**, *579*, 265−269.

(4) Letko, M.; Marzi, A.; Munster, V. Functional Assessment of Cell Entry and Receptor Usage for SARS-CoV-2 and Other Lineage B Betacoronaviruses. *Nat. Microbiol.* **2020**, *5*, 562−569.

(5) Guan, W.-J.; Ni, Z.-Y.; Hu, Y.; Liang, W.-H.; Ou, C.-Q.; He, J.-X.; Liu, L.; Shan, H.; Lei, C.-L.; Hui, D. S. C.; Du, B.; Li, L.-J.; Zeng, G.; Yuen, K.-Y.; Chen, R.-C.; Tang, C.-L.; Wang, T.; Chen, P.-Y.; Xiang, J.; Li, S.-Y.; et al. Clinical Characteristics of Coronavirus Disease 2019 in China. *N. Engl. J. Med.* **2020**, *382*, 1708−1720.

(6) Holshue, M. L.; DeBolt, C.; Lindquist, S.; Lofy, K. H.; Wiesman, J.; Bruce, H.; Spitters, C.; Ericson, K.; Wilkerson, S.; Tural, A.; Diaz, G.; Cohn, A.; Fox, L. A.; Patel, A.; Gerber, S. I.; Kim, L.; Tong, S.; Lu, X.; Lindstrom, S.; Pallansch, M. A.; et al. First Case of 2019 Novel Coronavirus in the United States. *N. Engl. J. Med.* **2020**, *382*, 929−936.

(7) Zhu, N.; Zhang, D.; Wang, W.; Li, X.; Yang, B.; Song, J.; Zhao, X.; Huang, B.; Shi, W.; Lu, R.; Niu, P.; Zhan, F.; Ma, X.; Wang, D.; Xu, W.; Wu, G.; Gao, G. F.; Tan, W. A Novel Coronavirus from Patients with Pneumonia in China, 2019. *N. Engl. J. Med.* **2020**, *382*, 727−733.

(8) Wang, F. S.; Zhang, C. What to Do Next to Control the 2019-NCoV Epidemic? *Lancet* **2020**, *395*, 391−393.

(9) Bai, Y.; Yao, L.; Wei, T.; Tian, F.; Jin, D.-Y.; Chen, L.; Wang, M. Presumed Asymptomatic Carrier Transmission of COVID-19. *JAMA* **2020**, *323*, 1406.

(10) Baud, D.; Qi, X.; Nielsen-Saines, K.; Musso, D.; Pomar, L.; Favre, G. Real Estimates of Mortality Following COVID-19 Infection. *Lancet Infect. Dis.* **2020**, DOI: 10.1016/S1473-3099(20)30195-X.

(11) Tellier, R. Review of Aerosol Transmission of Influenza A Virus. *Emerging Infect. Dis.* **2006**, *12*, 1657−1662.

(12) Yan, J.; Grantham, M.; Pantelic, J.; De Mesquita, P. J. B.; Albert, B.; Liu, F.; Ehrman, S.; Milton, D. K. Infectious Virus in Exhaled Breath of Symptomatic Seasonal Influenza Cases from a College Community. *Proc. Natl. Acad. Sci. U. S. A.* **2018**, *115*, 1081−1086.

(13) Lindsley, W. G.; Blachere, F. M.; Thewlis, R. E.; Vishnu, A.; Davis, K. A.; Cao, G.; Palmer, J. E.; Clark, K. E.; Fisher, M. A.; Khakoo, R.; Beezhold, D. H. Measurements of Airborne Influenza Virus in Aerosol Particles from Human Coughs. *PLoS One* **2010**, *5* (5), e15100.

(14) Loudon, R. G.; Roberts, R. M. Singing and the Dissemination of Tuberculosis. *Am. Rev. Respir. Dis.* **1968**, *98*, 297−300.

(15) CDC. Laboratory Performance Evaluation of N95 Filtering Facepiece Respirators, 1996. *Morb. Mortal. Wkly. Rep.* **1998**, *47*, 1045.

(16) Rosenstock, L. 42 CFR Part 84: Respiratory Protective Devices Implications for Tuberculosis Protection. *Infect. Control Hosp. Epidemiol.* **1995**, *16*, 529−531.

(17) NIOSH. Interim Guidance on Infection Control Measures for 2009 H1N1 Influenza in Healthcare Settings, Including Protection of Healthcare Personnel. *Miss. RN* **2009**, *71*, 13−18.

(18) Matsuyama, S.; Nao, N.; Shirato, K.; Kawase, M.; Saito, S.; Takayama, I.; Nagata, N.; Sekizuka, T.; Katoh, H.; Kato, F.; Sakata, M.; Tahara, M.; Kutsuna, S.; Ohmagari, N.; Kuroda, M.; Suzuki, T.; Kageyama, T.; Takeda, M. Enhanced Isolation of SARS-CoV-2 by TMPRSS2- Expressing Cells. *Proc. Natl. Acad. Sci. U. S. A.* **2020**, *117*, 7001−7003.

(19) Bałazy, A.; Toivola, M.; Adhikari, A.; Sivasubramani, S. K.; Reponen, T.; Grinshpun, S. A. Do N95 Respirators Provide 95% Protection Level against Airborne Viruses, and How Adequate Are Surgical Masks? *Am. J. Infect. Control* **2006**, *34*, 51−57.

(20) Wall, T. H.; Hansen, P. E. Filtering Web for Face Masks and Face Masks Made Therefrom. US3316904A, 1967.

(21) Ghosal, A.; Sinha-Ray, S.; Yarin, A. L.; Pourdeyhimi, B. Numerical Prediction of the Effect of Uptake Velocity on Three-Dimensional Structure, Porosity and Permeability of Meltblown Nonwoven Laydown. *Polymer* **2016**, *85*, 19−27.

(22) Kubik, D. A.; Davis, C. I. Melt-Blown Fibrous Electrets. US4215682A, 1980.

(23) Angadjivand, S. A.; Jones, M. E.; Meyer, D. E. Electret Filter Media. US6119691A, 1994.

(24) Barrett, L. W.; Rousseau, A. D. Aerosol Loading Performance of Electret Filter Media. *Am. Ind. Hyg. Assoc. J.* **1998**, *59*, 532−539.

(25) Ranney, M. L.; Griffeth, V.; Jha, A. K. Critical Supply Shortages — The Need for Ventilators and Personal Protective Equipment during the Covid-19 Pandemic. *N. Engl. J. Med.* **2020**, *382*, No. e41.

(26) van Doremalen, N.; Bushmaker, T.; Morris, D. H.; Holbrook, M. G.; Gamble, A.; Williamson, B. N.; Tamin, A.; Harcourt, J. L.; Thornburg, N. J.; Gerber, S. I.; Lloyd-Smith, J. O.; de Wit, E.; Munster, V. J. Aerosol and Surface Stability of SARS-CoV-2 as Compared with SARS-CoV-1. *N. Engl. J. Med.* **2020**, *382*, 1564−1567.

(27) Rutala, W. A.; Weber, D. J. *Guideline for Disinfection and Sterilization in Healthcare Facilities (2008)*; Centers for Disease Control and Prevention: Atlanta, GA, 2008; pp 1−163. https://www.cdc.gov/infectioncontrol/guidelines/disinfection/index.html (accessed 2020/03/28).

(28) Darnell, M. E. R.; Subbarao, K.; Feinstone, S. M.; Taylor, D. R. Inactivation of the Coronavirus That Induces Severe Acute Respiratory Syndrome, SARS-CoV. *J. Virol. Methods* **2004**, *121*, 85−91.

(29) Rabenau, H. F.; Cinatl, J.; Morgenstern, B.; Bauer, G.; Preiser, W.; Doerr, H. W. Stability and Inactivation of SARS Coronavirus. *Med. Microbiol. Immunol.* **2005**, *194*, 1−6.

(30) Chin, A. W. H.; Chu, J. T. S.; Perera, M. R. A.; Hui, K. P. Y.; Yen, H.-L.; Chan, M. C. W.; Peiris, M.; Poon, L. L. M. Stability of SARS-CoV-2 in Different Environmental Conditions. *Lancet Microbe* **2020**, DOI: 10.1016/S2666-5247(20)30003-3.

(31) Bergman, M. S.; Viscusi, D. J.; Heimbuch, B. K.; Wander, J. D.; Sambol, A. R.; Shaffer, R. E. Evaluation of Multiple (3-Cycle)

Decontamination Processing for Filtering Facepiece Respirators. *J. Eng. Fibers Fabr.* **2010**, *5*, 33−41.
(32) Xiao, H.; Song, Y.; Chen, G. Correlation between Charge Decay and Solvent Effect for Melt-Blown Polypropylene Electret Filter Fabrics. *J. Electrost.* **2014**, *72*, 311−314.
(33) Nazeeri, A. I.; Hilburn, I. A.; Wu, D.-A.; Mohammed, K. A.; Badal, D. Y.; Chan, M. H. W.; Kirschvink, J. L. An Efficient Ethanol-Vacuum Method for the Decontamination and Restoration of Polypropylene Microfiber Medical Masks & Respirators. *medRxiv*, 2020. https://www.medrxiv.org/content/10.1101/2020.04.12.20059709v1 (accessed 2020/04/28).
(34) Viscusi, D. J.; Bergman, M. S.; Eimer, B. C.; Shaffer, R. E. Evaluation of Five Decontamination Methods for Filtering Facepiece Respirators. *Ann. Occup. Hyg.* **2009**, *53*, 815−827.
(35) Yang, P.; Wang, X. COVID-19: A New Challenge for Human Beings. *Cell. Mol. Immunol.* **2020**, *17*, 555−557.
(36) Lindsley, W. G.; Martin, S. B.; Thewlis, R. E.; Sarkisian, K.; Nwoko, J. O.; Mead, K. R.; Noti, J. D. Effects of Ultraviolet Germicidal Irradiation (UVGI) on N95 Respirator Filtration Performance and Structural Integrity. *J. Occup. Environ. Hyg.* **2015**, *12*, 509−517.
(37) *Disinfection of Filtering Facepiece Respirators*; 3M: St. Paul, MN, 2020; pp 1−3.
(38) Price, A. Dp.; Cui, Y.; Liao, L.; Xiao, W.; Yu, X.; Wang, H.; Zhao, M.; Wang, Q.; Chu, S.; Chu, L. F. Is the Fit of N95 Facial Masks Effected by Disinfection? A Study of Heat and UV Disinfection Methods Using the OSHA Protocol Fit Test. *medRxiv*, 2020. https://www.medrxiv.org/content/10.1101/2020.04.14.20062810v1 (accessed 2020/04/28).
(39) Bergman, M. S.; Viscusi, D. J.; Zhuang, Z.; Palmiero, A. J.; Powell, J. B.; Shaffer, R. E. Impact of Multiple Consecutive Donnings on Filtering Facepiece Respirator Fit. *Am. J. Infect. Control* **2012**, *40*, 375−380.

https://dx.doi.org/10.1021/acsnano.0c03597
ACS Nano XXXX, XXX, XXX−XXX